Surface spin-flop and discommensuration transitions in antiferromagnets

C. Micheletti
International School for Advanced Studies (SISSA) and INFM, Via Beirut 2-4, 34014 Trieste, Italy and The Abdus Salam Centre for Theoretical Physics, Trieste, Italy

R. B. Griffiths
Physics Department, Carnegie-Mellon University, Pittsburgh, Pennsylvania 15213

J. M. Yeomans
Theoretical Physics, Oxford University, 1 Keble Road, Oxford OX1 3NP, United Kingdom

(Received 11 September 1998)

Phase diagrams as a function of anisotropy D and magnetic field H are obtained for discommensurations and surface states for an antiferromagnet in which H is parallel to the easy axis, by modeling it using the ground states of a one-dimensional chain of classical XY spins. A surface spin-flop phase exists for all D, but the interval in H over which it is stable becomes extremely small as D goes to zero. First-order transitions, separating different surface states and ending in critical points, exist inside the surface spin-flop region. They accumulate at a field H' (depending on D) significantly less than the value $H_{\rm SF}$ for a bulk spin-flop transition. For $H'<H<H_{\rm SF}$ there is no surface spin-flop phase in the strict sense; instead, the surface restructures by, in effect, producing a discommensuration infinitely far away in the bulk. The results are used to explain in detail the phase transitions occurring in systems consisting of a finite, even number of layers.
[S0163-1829(99)02309-7]

I. INTRODUCTION

It has been known for a long time that if an antiferromagnet with suitable anisotropy is placed in an external magnetic field H parallel to the easy axis (the axis along which the spins are aligned, in opposite directions on different sublattices, in zero magnetic field) and the field strength is increased, a first-order transition will occur[1] in which the spins are realigned in directions (approximately) perpendicular to the applied field, but with a component along the field direction. The transition to this *spin-flop* phase occurs when H is equal to a spin-flop field $H_{\rm SF}$, whose value depends on the exchange energy and the anisotropy. As H continues to increase beyond $H_{\rm SF}$, the spins on the two sublattices rotate towards the field direction till eventually, if the field is sufficiently large, they are parallel to each other in a ferromagnet structure.

In 1968 Mills[2] proposed that in an antiferromagnet with a free surface, spins near the surface could rotate into a flopped state at a field $H'_{\rm SF}$ significantly less than $H_{\rm SF}$. This *surface spin-flop* (SSF) problem was later studied by Keffer and Chow,[3] who found a transition at $H'_{\rm SF}$, but to a state having a character rather different than that proposed by Mills. Interest in this problem was recently rekindled through experimental work on layered structures consisting of Fe/Cr(211) superlattices.[4,5] If the thickness of the Cr layers is chosen appropriately, adjacent Fe blocks are coupled antiferromagnetically, and thus in zero magnetic field they exhibit an antiferromagnetic structure in which the magnetization of each layer is opposite to that of the adjoining layers. Applying an external magnetic field parallel to the layers can give rise to phase transitions in which the magnetization in certain layers rotates or reverses its direction, and the results found experimentally depend upon whether the number of Fe layers is even or odd. The experimental work has motivated a number of theoretical and numerical studies of finite and semi-infinite systems.[4–9] Most of these have found evidence for the existence of SSF states.

In the present paper we address the issue of the existence of SSF phases and some related topics by studying the properties of the ground states of chains of antiferromagnetically coupled classical XY spins, each spin variable represented by an angle θ between 0 and 2π, subject to a uniaxial anisotropy D as well as to an external magnetic field H, as a function of D and H. One can think of θ as the direction of the magnetization in an Fe layer in a superlattice, or of the average magnetization in a layer of an antiferromagnet containing spins belonging to one type of sublattice. Minimizing the energy of a one-dimensional model then corresponds to minimizing the free energy of a three-dimensional layered system, provided fluctuations inside the layers do not have a drastic effect. This means that the model we consider here is, in its essentials, equivalent to those used in previous studies. It allows us to come to some fairly definite conclusions about SSF phases in semi-infinite systems, and about the behavior of systems containing a finite number of layers. Our principal conclusions were published previously in a short report;[10] the present paper contains the complete argument, and supplies a number of additional details.

In order to understand the properties of finite and semi-infinite chains, it is helpful to begin with an infinite chain and a defect structure known as a ''discommensuration'' (or ''soliton'' or ''kink''), which can occur in both the antiferromagnetic and the spin-flop phases. In Sec. II we work out the properties of the discommensurations of minimum energy in the antiferromagnetic ground state of the XY chain.

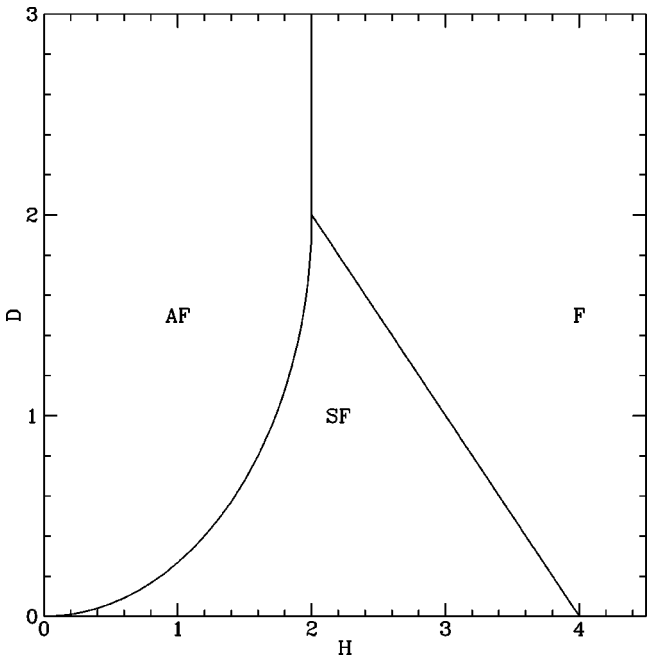

FIG. 1. Phase diagram for an infinite chain. The AF, F, and SF regions are occupied by the antiferromagnetic, ferromagnetic, and spin-flop phases respectively.

Using these results, we obtain, in Sec. III, a phase diagram for surface phase transitions in a semi-infinite chain. Both discommensurations and surface phase transitions are essential for understanding the properties of finite chains. These are discussed in Sec. IV, where we provide a comprehensive and detailed explanation of the complicated series of transitions found in chains containing an even number of spins.

The numerical procedures we used to study the phase diagram are described in Secs. II and III, and a certain number of analytic results are derived in Sec. V. The concluding Sec. VI provides a summary, and notes some topics which still need to be studied.

II. INFINITE CHAIN

We consider an infinite chain of classical XY spins described by the Hamiltonian

$$\mathcal{H}=\sum_{i=-\infty}^{\infty}\left\{\cos(\theta_i-\theta_{i+1})-H\cos\theta_i+\frac{D}{4}[1-\cos(2\theta_i)]\right\}, \tag{1}$$

where the antiferromagnetic exchange coefficient has been taken as the unit of energy, θ_i is the angle between the direction of the ith spin and the external magnetic field H, and D is a twofold spin anisotropy. Our aim is to identify the zero-temperature phases of this system, that is, those which minimize the energy. Minimizing the energy of a one-dimensional system corresponds to minimizing the free energy of a layered three-dimensional system when the fluctuations within each individual layer are not playing an important role, as is the case for the Fe/Cr superlattices mentioned in Sec. I.

The phase diagram of the system consists of three separate regions, as shown in Fig. 1. For $D>2$, the line $H=2$ separates the ferromagnetic (F) configuration, with all the spins parallel to the field, from the antiferromagnetic (AF) one with the spins alternating between 0 and π, parallel and antiparallel to the field. Along the AF:F boundary the ground state is infinitely degenerate since it is possible to flip any number of nonadjacent spins in the F chain with no change in energy.

For $D<2$ and intermediate values of H, the ground state no longer corresponds to spins in the Ising positions, θ_i equal 0 or π, but is a spin-flop (SF) phase in which the spins alternate between $+\phi$ and $-\phi$, where

$$\cos\phi=H/(4-D). \tag{2}$$

The spin-flop region extends between the boundaries $H=\sqrt{D(4-D)}$ and $H=4-D$ which are first and second order, respectively.[11]

We now consider the case when an infinite chain is constrained by suitable boundary conditions to include a discommensuration (for detailed studies of discommensurations in Frenkel-Kontorova models see, for example, Refs. 12–15). The study of the discommensuration phase diagram is important because it helps us to understand the minimal energy configurations observed both in semi-infinite and finite systems. A discommensuration is a defect which can arise in a periodic phase whose period is two or greater. In particular, the AF ground state has period two and is degenerate: for one ground state $\theta_i=0$ for i even and π for i odd; for the other, $\theta_i=\pi$ for i even and 0 for i odd. A discommensuration results if one requires that a single configuration $\{\theta_i\}$ approaches one of these ground states as i tends to $-\infty$ and the other as i tends to $+\infty$; for instance,

$$\theta_{2n}\to 0, \quad \theta_{2n+1}\to\pi \text{ as } n\to+\infty,$$

$$\theta_{2n}\to\pi, \quad \theta_{2n+1}\to 0 \text{ as } n\to-\infty. \tag{3}$$

The defect energy of a discommensuration is the difference between the energy of the configuration containing the discommensuration and the energy of the corresponding ground state. Since both of these energies are infinite for an infinite chain, a proper definition requires some care; see, e.g., Ref. 16. We are interested in discommensurations which, for a given D and H, minimize this energy; they constitute what we call the discommensuration phase diagram. It is convenient to start by considering the limiting case $D=\infty$, where the spins are constrained to lie along the Ising positions. For $0<H<2$ the discommensuration of minimum energy is a configuration in which two successive spins someplace in the middle of the chain are parallel to the field H:

$$\ldots,0,\pi,0,\pi,0,0,\pi,0,\pi,\ldots\ . \tag{4}$$

In the following we will use the notation AF′ to label this phase. When $H=2$, due to the absence of further-than-nearest-neighbor interactions, there is not a unique minimum-energy discommensuration associated with the AF phase. One can have any arbitrary even number of spins aligned with the field, not just two, as in Eq. (4), and other, more complicated defects are possible. The ferromagnetic ground state for $H\geqslant 2$ has period one and is nondegenerate, so there are no discommensurations.

As the spin anisotropy D decreases from infinity, lower energies may occur if in a discommensuration the spins are not limited to the Ising values 0 and π. For these cases it is difficult to find an explicit analytic form for the minimum energy discommensuration, and one has to use numerical techniques to tackle the problem. The numerical procedure that we have adopted relies on the method of effective potentials,[17,18] which is very efficient for obtaining the ground state of models with short-range interactions and discretized variables. The main advantage of this method is that it yields the true ground state, rather than some metastable one. The main disadvantage for our problem is that it requires the spin variables to be discretized: they can take on only a finite number of values. We generally used a discretization grid in which each θ_i is an integer times $2\pi/1400$. To overcome the effects of the discretization we first fixed the anisotropy at some intermediate value, typically $D\approx 0.6$, then used the Chou-Griffiths algorithm[17] to identify minimal energy states of different phases for the system of discretized spins, and, finally, employed the equilibrium equations,

$$\frac{\partial \mathcal{H}}{\partial \theta_i}=0, \tag{5}$$

for continuous spins in order to refine the configurations obtained using discretized spins. The phase boundaries located by comparing the energies of neighboring phases, calculated using the refined configurations, were then followed as the value of D was changed in small steps, while the spin configurations were updated using Eq. (5). The location of the phase boundaries was then checked against those obtained starting with finer discretization grids. We established that, using a discretization of $2\pi/1400$, the error in the location of the boundary, ΔH, was in the range of 10^{-8}–10^{-9} throughout the range of D values we studied. The procedure just described was used to find minimum energy configurations of a ring of spins (periodic boundary conditions) of length L with L odd, so as to produce a configuration containing a discommensuration. When L is large (we used $L\leqslant 31$) compared to the size of the discommensuration, this is practically the same as studying the minimal energy discommensuration in an infinite chain.

The numerical results are summarized in the discommensuration phase diagram in Fig. 2. There are, of course, no discommensurations in the F phase. As for the SF phase, our numerical results showed a smooth variation of spin angles with D and H, and consequently no phase transitions. However, various phase transitions were identified for AF phase discommensurations. In the AF′ region, Fig. 2, the spins in the minimum energy discommensuration stay locked in their $D=\infty$ positions. The persistence of this Ising spin locking for finite values of the anisotropy is a rather common feature in models with twofold spin anisotropy.[19–21] Here it has the consequence that the multiphase degeneracy encountered at the point ($H=2$, $D=\infty$) persists throughout the locus ($D\geqslant 2$, $H=2$).

For values of D lying below the lower boundary of AF′, but still inside the AF region in Fig. 2, ''flopped'' discommensurations of different length have lower energies than the Ising discommensuration (4). A flopped discommensuration of type $\langle 2m\rangle$ consists of a ''core'' of $2m$ spins in which the spin configuration resembles that in a bulk spin-flop phase, located between ''tails,'' each of which rapidly reverts to the configuration of the corresponding AF phase with increasing distance from the core (see Fig. 3). One can think of the region where the core changes into the tail as an ''interface'' between the AF phase out in the tail and the SF phase in the core. From this perspective, the discommensuration consists of a pair of interfaces, AF-SF and SF-AF, bounding the SF core. As D decreases, these interfaces broaden, making the distinction between the ''tails'' and the ''core'' less clear, but we continue to use the same label $\langle 2m\rangle$ for the discommensuration which evolves continuously from the one with a clearly-defined core of size $2m$ at larger D.

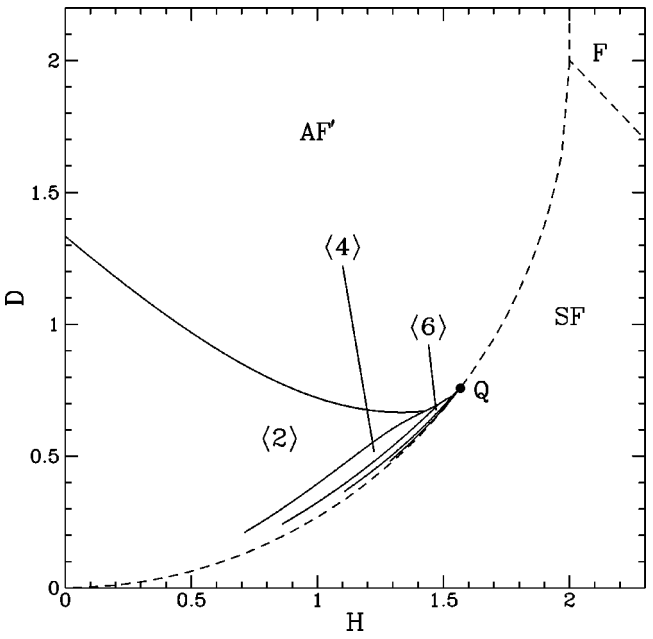

FIG. 2. Discommensuration phase diagram for an infinite chain. The dashed phase boundaries correspond to phase transitions in the discommensuration-free chain, the solid lines in Fig. 1.

An analytic calculation, see Sec. V, shows that the equation for the second-order transition between AF′ and $\langle 2\rangle$ in Fig. 2 is

$$(D+H-1)^{-1}=5/3+D-H, \tag{6}$$

in good agreement with our numerical calculations, and those in Ref. 22 when $H=0$. At low values of H, the discommensuration $\langle 2\rangle$ has the lowest energy, but upon approaching the bulk AF:SF phase boundary, one finds a sequence of phase transitions to $\langle 4\rangle$,$\langle 6\rangle$, ... as H increases,

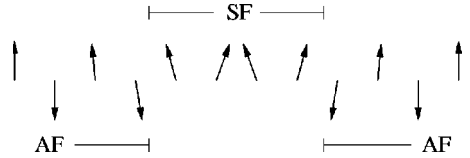

FIG. 3. Schematic representation of phase $\langle 4\rangle$ for moderate values of the spin anisotropy. The phase can be regarded as resulting from merging a portion of the spin-flop phase (SF) with two semi-infinite antiferromagnetic chains (AF). The spins nearest the AF-SF and SF-AF interfaces are expected to relax from their ideal AF or SF angles.

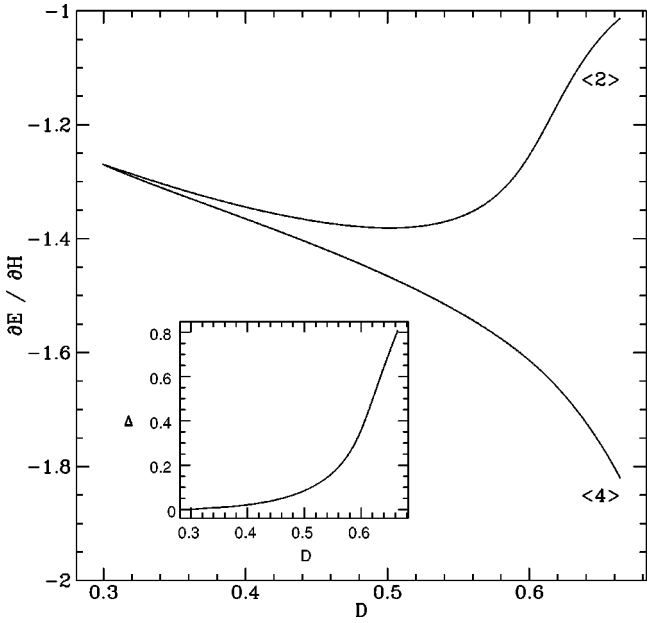

FIG. 4. Plot of the derivative of the energy with respect to field in the two neighboring phases, $\langle 2\rangle$,$\langle 4\rangle$ along their common boundary, for a ring of 17 spins. The inset shows the difference Δ of the two derivatives.

as shown in Fig. 2. Our numerical procedures found values of $2m$ up to 14, and we were able to trace the first-order lines separating the different $\langle 2m\rangle$ phases down to a value of D between 0.1 and 0.4. For smaller values of D, the difference Δ of the energy derivatives $\partial E/\partial H$ in two neighboring phases was no longer sufficient to allow us to distinguish the phases numerically and locate the phase boundary. See the example in Fig. 4. However, we found no evidence that these lines terminate in critical points. The smooth decrease of Δ shown in the inset of Fig. 4 contrasts with what one might expect at a critical point (as in Fig. 8). Therefore, it seems plausible to assume that the $\langle 2m\rangle$:$\langle 2m+2\rangle$ boundaries persist all the way down to $D=0$.

The sequence of transitions associated with a broadening of the discommensuration can be understood in the following way. The defect energy of a discommensuration can be thought of as the sum of the energy required to produce a pair of AF-SF and SF-AF interfaces infinitely far apart, an interaction energy between the interfaces which we assume is positive and rises rapidly as they approach each other, and a ''bulk'' contribution proportional to the size of the core, arising from the fact that in the AF part of the phase diagram, the SF phase is metastable. In terms of which discommensuration has the lowest energy, the interface repulsion obviously favors a large core, and the metastable ''penalty'' a small core. The actual size will represent some compromise between the two. Upon approaching the AF:SF boundary, the metastable penalty goes to zero, so the discommensuration of minimum energy should become larger and larger. Hence, one expects the $\langle 2m\rangle$:$\langle 2m+2\rangle$ boundary to approach the AF:SF transition line as $m\to\infty$. This is consistent with our numerical calculations, and in agreement with the predictions of Papanicolaou.[22] (Note, however, that these transitions reflect the discrete nature of the spin chain and therefore are absent in the continuum approximation employed in Ref. 22 for small spin anisotropy.) The triple points at which the phases AF′,$\langle 2m\rangle$ and $\langle 2m+2\rangle$ meet tend to an accumulation point, Q, located at $H\approx 1.58$, $D\approx 0.78$. This should be the point at which the energy to create a pair of AF-SF and SF-AF interfaces infinitely far apart is equal to the energy of an Ising discommensuration.

III. SEMI-INFINITE CHAINS

We now consider the surface states of a semi-infinite chain. The Hamiltonian for the system is the same as Eq. (1) but with the sum extending only over non-negative values of i ($i=0$ denotes the surface site):

$$\mathcal{H}=\sum_{i=0}^{\infty}\left\{\cos(\theta_i-\theta_{i+1})-H\cos\theta_i+\frac{D}{4}[1-\cos(2\theta_i)]\right\}. \tag{7}$$

It is useful to think of semiinfinite chains as obtained by cutting an infinite chain in two. Removing a bond in the infinite chain without allowing the spins to move will give two semi-infinite chains that we shall term unreconstructed. If the spins of the unreconstructed chains are then allowed to relax, a rearrangement of the spins near the surface may take place, as illustrated in Fig. 5, which lowers the energy. Notice that even though the total energy of the semi-infinite chain is infinite, *changes* in the energy when a configuration is modified near the surface (or in a way such that the modifications decrease sufficiently rapidly with increasing distance from the surface) are well defined. We want to consider surface states which minimize the energy in the sense that no local modifications of the configuration near the surface can decrease the energy.

The task of finding the reconstructed surface of minimum energy is, in general, not simple (except when all the spins in the chain are subject to the Ising locking). To identify the minimal energy surface states we used numerical algorithms based on effective potential methods that, as mentioned earlier, require a discretization of the spin variables at each site. It is important to notice that, since the θ_i's are constrained to take on only discrete values, after a finite distance, or ''penetration depth'' l from the surface the spins will be *exactly* in the discretized positions corresponding to a doubly infinite chain or an unreconstructed surface. Configurations for the infinite chain were obtained using the Floria-Griffiths algorithm[23] which, within the limits of the discretization, yields the exact ground state. Next, the Chou-Griffiths algorithm[17] with its successive iterations was used to generate reconstructed surface configurations $\{\theta_0,\theta_1,\ldots,\theta_l\}$.

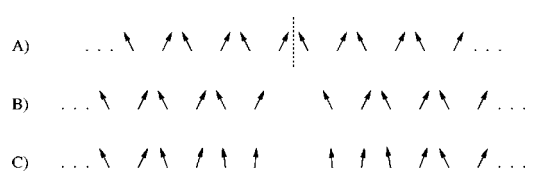

FIG. 5. Cutting an infinite chain in two (a) while keeping the spins ''frozen'' results in two semi-infinite chains with unreconstructed surfaces (b). Allowing the spins to relax to positions which minimize the energy typically results in reconstruction of the surface (c), a rearrangement of the spins nearest the surface.

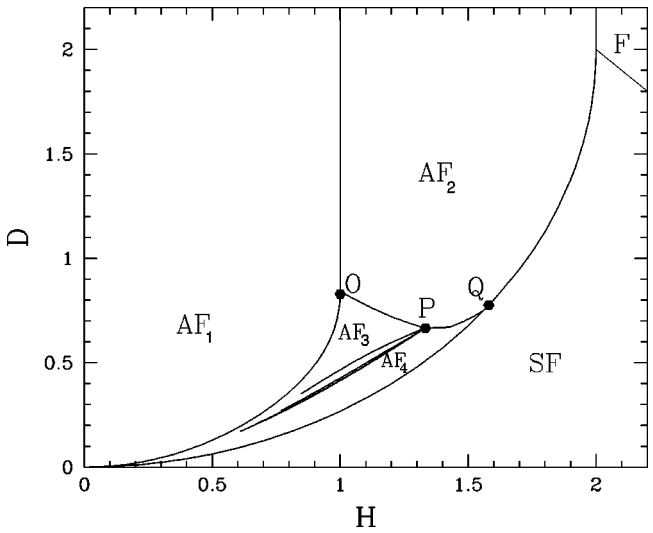

FIG. 6. Phase diagram for a semi-infinite chain with a *B*-type surface. More details of the AF_3 region are visible in Fig. 7.

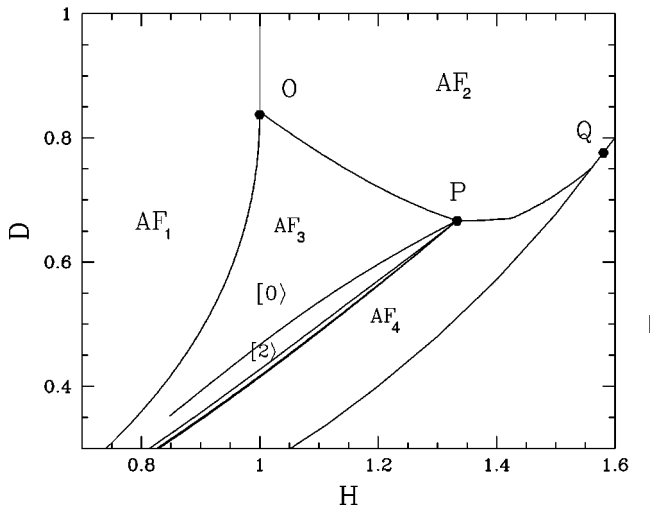

FIG. 7. Detail of the phase diagram for a semi-infinite chain with a *B*-type surface.

This should give the exact configuration minimizing the surface energy for the discrete spins. However, in practice we had to limit l to a maximum value $l_{\max}$ no larger than 50; thus the method could not yield the correct configuration for a larger penetration depth. The phase boundaries were then identified as explained in the previous section.

The resulting phase diagram is shown in Fig. 6. Throughout the F region the minimum energy surface states are simply the unreconstructed surfaces; it is easy to see that making any changes will increase the energy. In the SF region, since the ground state of the infinite chain has period two, there are two unreconstructed surfaces. Each of them undergoes a reconstruction in which the spins nearest the surface tilt towards the magnetic-field direction, as in Fig. 5(c). However, this change in spin direction occurs continuously as a function of H and D, and so no surface phase transitions are observed inside the SF region.

Next consider the AF part of the phase diagram. Again there exist two possible surface states, A and B, whose unreconstructed versions, A_u and B_u, have surface spins parallel ($\theta_0=0$) or opposite ($\theta_0=\pi$) to the field direction:

$$A_u=\{0,\pi,0,\pi,0,\pi,\ldots\}, \tag{8}$$

$$B_u=\{\pi,0,\pi,0,\pi,0,\ldots\}. \tag{9}$$

A surface will be said to be of type A (B) if the spin configuration tends to that of $A_u(B_u)$ far from the surface.

Throughout the AF region of the phase diagram, the minimum energy surface of type A is the unreconstructed A_u. However, the B-type surface shows a number of different structures in different parts of the AF region, as indicated in Figs. 6 and 7. In region AF_1 the unreconstructed surface B_u has the lowest energy. In region AF_2, which meets AF_1 along a line $H=1$ for D larger than the value at O, it is energetically favorable to flip the surface spin so that it points along the field direction, and there is a set of degenerate (equal minimum energy) reconstructed surfaces

$$[0\rangle=0,0,\pi,0,\pi,0,\pi\ldots, \quad [2\rangle=0,\pi,0,0,\pi,0,\pi\ldots, \tag{10}$$

and so forth, where $[2n\rangle$ consists of $2n$ spins $0,\pi,\ldots$ in an antiferromagnetic arrangement, followed by two spins parallel to the field, and then the bulk antiferromagnetic phase. One can think of this reconstructed surface as an Ising discommensuration, whose core consists of two adjacent spins with $\theta_i=0$, located a distance $2n$ from the surface. Because the ''tails'' of this discommensuration have zero length, it does not interact with the surface, and its energy is independent of its distance from the surface. While this degeneracy persists throughout the AF_2 region, along the line $D\geqslant 2, H=2$ the degeneracy is even greater: the set of minimum energy surface states includes cases where the number of consecutive spins pointing along the field is not limited to 2 but can attain any even number, e.g., $\{0,0,0,0,\pi,0,\pi\ldots\}$ or $\{0,\pi,0,\pi,0,0,0,0,0,0,\pi,0,\pi\ldots\}$. Incidentally, we note that these degeneracies are somewhat artificial in that they would be lifted by introducing weak longer-range interactions in the Hamiltonian (7).

In the AF_3 region of Fig. 6 the B-type surface again reconstructs, but the spin anisotropy is sufficiently low that the spins unlock from the Ising angles. As in the AF_2 region, one can think of the surface state as consisting of a discommensuration located a finite distance from the surface, but now this discommensuration is of the flopped type with a core of length of 2, and tails extending out on either side of the core. We again employ the notation $[2n\rangle$ for the surface state with $2n$ spins to the left of the core, that is, in the tail extending to the surface. Because of this tail, the discommensuration interacts with the surface, and the minimum surface energy occurs for a specific value of $2n$, depending upon D and H. Thus, in AF_3, one finds genuine spin-flop surface states. As H increases, the discommensuration moves further from the surface. It does this, at least when D is large, discontinuously in steps of 2, via a series of first-order phase transitions, some of which are shown in Fig. 7, where they extend leftwards from the point P. For smaller values of D, the edges of the core are not as well defined, and it is more difficult to associate the $[2n\rangle\rightarrow[2n+2\rangle$ transitions with a discontinuous jump of the discommensuration. Numerically we have seen states with $2n$ up to 14, and our results are consistent

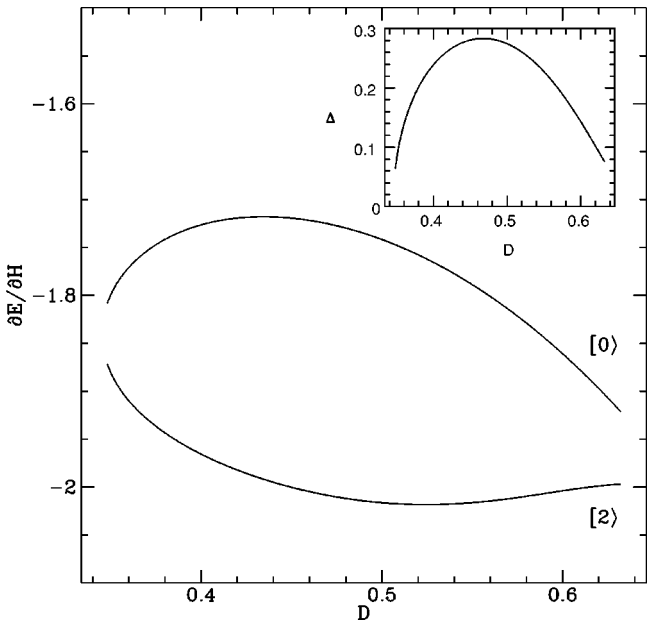

FIG. 8. Plot of the derivative of the energy with respect to field in the two neighboring phases $[0\rangle$ and $[2\rangle$ along their common boundary, using 50 spins in the surface layer. The inset shows the difference Δ of the two derivatives.

with n tending to infinity at the right side of the AF_3 region, which our analytic calculations (Sec. V), in agreement with Ref. 6, show to be the line

$$D=\sqrt{1+H^2}-1. \tag{11}$$

The upper boundary of the AF_3 region extending from O to P is a continuous (second-order) transition. One can think of it as the limit of stability of the Ising surface phase $[0\rangle$ as D decreases inside AF_2. An analytic calculation, Sec. V, shows that the implicit equation for the boundary is

$$(2+D-H-1/a)^{-1}=2+D+H-a,$$

$$a:=H+D+1/(1-H-D). \tag{12}$$

Thus the point P, where all the phases $[2n\rangle$ come together, lies at $H=4/3$, $D=2/3$, the intersection of Eqs. (11) and (12). Both Eqs. (11) and (12) agree with our numerical results.

We find that the first-order lines extending downwards and leftwards from P in Fig. 7, separating phases $[2n\rangle$ from $[2n+2\rangle$, end in critical points as D decreases. This is clearly visible in the example in Fig. 8, which shows the typical behavior of the energy derivatives of two neighboring phases along their coexistence line. Near a critical point $D=D_c$ one expects Δ to vary as $\sqrt{D-D_c}$, in qualitative agreement with what we observed. The larger the value of n, the further the first-order line extends towards the origin of the H,D plane, but presumably for any finite value of n the difference between the phases $[2n\rangle$ and $[2n+2\rangle$ eventually disappears at some finite value of D. Because this value decreases with increasing n, it is plausible that the corresponding critical points accumulate at the origin.

As is evident in Fig. 6, the region AF_3 becomes extremely narrow as D decreases. The left boundary approaches a parabola $D=0.5H^2$ to within numerical precision, which is asymptotically the same as Eq. (11). We nonetheless believe that the width of AF_3 remains finite as long as $D>0$. Numerical evidence for this is shown in Fig. 9 where the value of the surface spin, θ_0, at the left edge of the AF_3 region (that is for H just large enough to produce the surface spin-flop phase) is plotted as a function of D. The results are for $l_{\max}=34$ spins in the surface layer (see the description of the numerical approach given above). Below $D=0.05$ the results become unreliable because $l_{\max}$ is too small, as we can tell by carrying out calculations for different values of $l_{\max}$. However, extrapolating from larger values of D indicates that as D goes to zero, θ_0 tends to a value near $\pi/3$ or 60°, showing that even for very small D the discommensuration at the threshold field is still a finite distance from the surface. This situation is quite distinct from that in region AF_1, where $\theta_0=\pi$, and in AF_4, discussed below, where $\theta_0=0$.

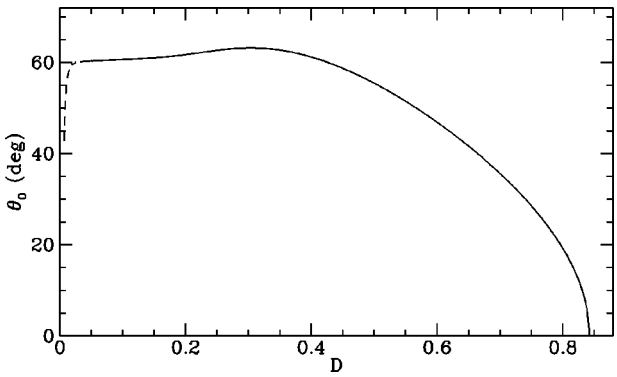

FIG. 9. Surface spin θ_0 along the left edge of the AF_3 region as a function of anisotropy D. The surface layer consisted of 34 spins, and the behavior of the curve at low D (dashed) is affected by finite-size effects in the numerical calculations.

Between AF_3 and the AF:SF bulk phase boundary lies region AF_4, see Figs. 6 and 7, in which the flopped discommensuration is repelled by the surface, so that its minimum energy location is in the bulk infinitely far away from the surface, as noted in Ref. 6. Thus there is no minimum-energy reconstructed B surface, or, properly speaking, a ''surface spin-flop phase'' in region AF_4. It seems better to identify AF_4, thought of as part of the B-type surface phase diagram, as a ''discommensuration phase,'' since the minimum energy surface will always be of the A-type, with the surface spin $\theta_0=0$.

In Fig. 10 the discommensuration phase diagram for the infinite chain (Fig. 2), represented by dashed lines, is superimposed on the B-type surface diagram for the semi-infinite chain, represented by solid lines, in the vicinity of points P and Q, which are common to both diagrams, as is the broken line (shown dashed) from P to Q. Note that the OP line of the surface diagram, Fig. 7, lies above the lower boundary of the AF' region of the discommensuration phase diagram in Fig. 2. Thus to the left of P, for $H<4/3$, as D decreases the reconstructed B-type surface phase changes from Ising to a flopped form before the corresponding change is energetically favorable for the bulk discommensuration.

In addition, Fig. 10 shows that the part of the H,D plane corresponding to $\langle 2m\rangle$ in the discommensuration phase diagram, Fig. 2, for $2m\geq 4$ lies entirely inside the AF_4 region of

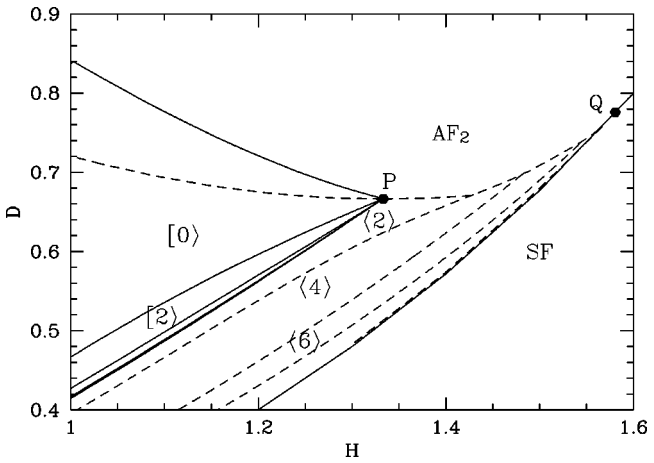

FIG. 10. Discommensuration phase diagram (Fig. 2), using dashed lines, superimposed on the phase diagram for a semi-infinite chain with a *B*-type surface (Fig. 7), using solid lines, in the vicinity of the point *P*. The broken line connecting *P* with *Q* is part of both phase diagrams.

Fig. 6 (and 7) for the surface phase diagram. This is consistent with our observation that as long as the discommensuration is a finite distance from the surface, in the AF_3 region, it is always of the type $2m=2$. Thus as H increases, it is only *after* the discommensuration has moved infinitely far from the surface, and thus has no influence on the surface phase diagram, that its core begins to broaden.

In retrospect it seems likely that the broadening of the SSF transition mentioned in the abstract of Ref. 3 actually refers to broadening of the bulk discommensuration which, as noted above, occurs as H approaches the AF:SF boundary inside region AF_4. It appears that no work prior to ours has correctly identified the stable SSF phase at small values of D, characterized when it first appears with increasing H by a surface spin with a value very near 60° (Fig. 9). The narrowness of the AF_3 region for small D may be why it was overlooked.

IV. FINITE CHAIN

We now move on to consider the case of a chain of finite length L. Since a surface reconstruction can occur at both ends of the chain, and it is also possible for a discommensuration to be present in the interior of the chain, we write its total energy in the form

$$E_L = L\epsilon + E_s^L + E_s^R + E_d, \tag{13}$$

where ϵ is the bulk energy, the ground-state energy per spin for an infinite chain, E_s^L and E_s^R are the energies of the left and right surfaces, respectively, and E_d is the energy of a discommensuration in the chain (if present). Minimizing the total energy for fixed L is equivalent to finding the spin configuration that minimizes $E_s^L + E_s^R + E_d$.

In writing Eq. (13), L was assumed to be sufficiently large that the interaction between the two ends of the chain, and between each end and the discommensuration, if present, can be neglected. For any given L this condition can always be satisfied by choosing a large enough value for the spin anisotropy. Outside the range of D for which Eq. (13) holds, the behavior of the system will depend strongly on the actual length of the chain. Since we are not interested in L-dependent features of the phase diagram, apart from whether L is even or odd, we shall assume that L is sufficiently large to justify the use of Eq. (13).

From the discussion presented in the previous sections one can predict that a finite chain will not undergo any phase transition for values of D and H inside the SF and F regions. On the other hand, it can also be anticipated that the behavior of the chain in the AF region will be rather complicated. As noted in Refs. 4,5,7, the behavior of the chain for values of D and H in the AF region changes dramatically according to whether the length of the chain is even or odd.

If L is odd, both ends of the chain have to be of the same type, *A* or *B*, unless a discommensuration is present. Having two *A*-type surfaces gives a lower energy than two *B*-type surfaces, because the former results in a net magnetization in the direction of the field, and the latter a net magnetization opposite to the field. Similar considerations show that throughout the AF region it is energetically unfavorable to insert a dislocation, thus producing one *A*-type and one *B*-type surface. Hence for odd L, the minimum energy corresponds to two (unreconstructed) *A*-type surfaces at either end of the chain, and no discommensurations.

On the other hand, when L is even, the two surfaces have to be of different types, unless a discommensuration is present. The analysis of Sec. II has shown that discommensurations are not favored energetically outside region AF_4. Thus, for D and H falling in region AF_1 or AF_3, one expects one surface of type *A* and the other of type *B*. Moreover, from the results of Sec. III, we expect that in region AF_1 the *B* surface remains unreconstructed, whereas surface spin-flop states should be observed in AF_3 owing to the reconstruction of the *B*-type end of the chain. The *A*-type end of the chain remains, of course, in its unreconstructed state. Next, in region AF_4 the energy is minimized using two *A*-type surfaces and a discommensuration, which lies at the center of the finite chain because it is repelled by both surfaces. Finally, in AF_2, because of the degeneracy due to the Ising spin locking, one has either a reconstructed *B*-type surface or a discommensuration, depending upon what one wants to call it, and an *A*-type surface at the other end of the chain.

Consequently, if D is smaller than the value corresponding to point *P* in Fig. 7, we expect a finite system with even L to undergo the following set of transitions with increasing H. At $H=0$, Fig. 11(a), there are unreconstructed surfaces of types *A* and *B* at opposite ends of the chain. When H reaches the threshold for the formation of an SSF phase, the *B*-type surface restructures discontinuously, (b) to form a type $\langle 2\rangle$ discommensuration which then, as H increases, moves towards the center of the chain in a series of discontinuous steps, (c) and (d), some of which may be continuous if D is smaller than the value for the corresponding critical point, see Sec. III.

The discommensuration will reach the center of the chain, Fig. 11(d), when H is close to the threshold for the AF_4 or discommensuration region in Fig. 6. Further increases of H will lead to a broadening of the discommensuration, with $\langle 2m\rangle$ going through the sequence $\langle 2\rangle,\langle 4\rangle,\langle 6\rangle,\ldots$ of Fig. 2; see Figs. 11(d) to 11(g). While these transitions are likely to be discontinuous for larger values of D, it may be hard to

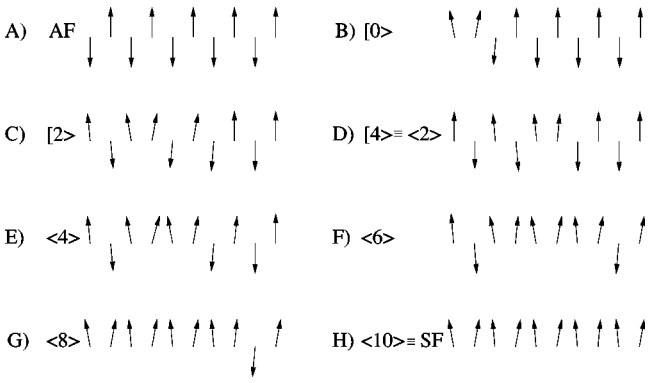

FIG. 11. Schematic representation of the series of different phases encountered in a chain of 10 spins for increasing values of H.

see the discontinuities when D is small. The center of the $\langle 2m\rangle$ discommensuration in Fig. 11 does not fall at the precise center of the chain when m is even; the offset is needed so that the surface spins can both be (approximately) parallel, rather than antiparallel, to the field direction. (For $L=12$ the offset occurs when m is odd.)

The AF-SF and SF-AF interfaces on either side of the core move outwards as the discommensuration expands, and eventually they reach the surfaces of the chain, Fig. 11(g), at a field very close to that required to produce the bulk spin-flop transition. At still higher fields the entire chain can be thought of as being in the bulk spin-flop phase, with appropriate (reconstructed) surface configurations corresponding to this phase. Sufficiently large values of H will eventually force all of the spins into the ferromagnetic configuration $\theta_i=0$.

The scenario just described is basically consistent with previous numerical studies, including two that have appeared quite recently,[8,9] and our own numerical work. Thus Fig. 12 shows the magnetic susceptibility $\chi=\partial M/\partial H, M$ the magnetization, for a chain of $L=22$ spins when $D=0.5$. The spikes appearing in Fig. 12 should be Dirac delta functions. Here they appear to have a finite height because of the finite incremental step δH chosen for the numerical calculation. The first spike in Fig. 12 (for $H\approx 0.9$) signals the transition from

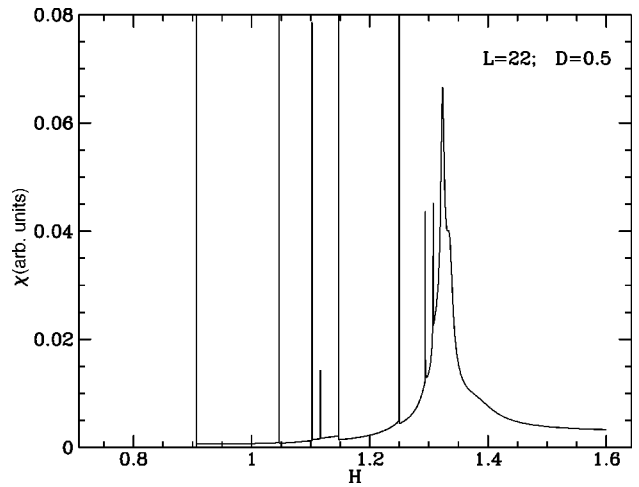

FIG. 12. Plot of the susceptibility (in arbitrary units) for a chain of 22 spins for $D=0.5$.

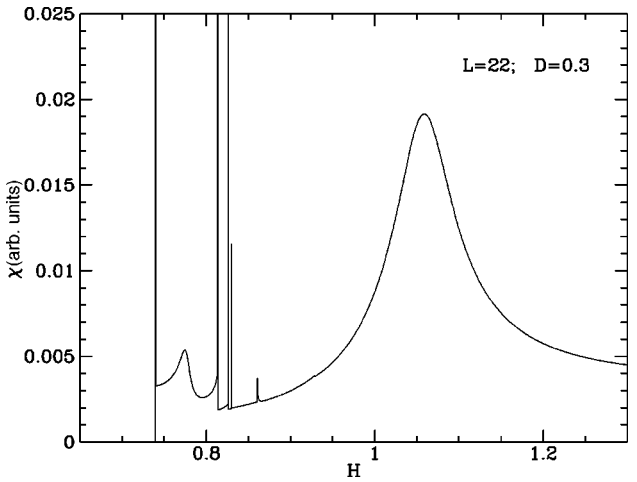

FIG. 13. Plot of the susceptibility (in arbitrary units) for a chain of 22 spins for $D=0.3$.

the AF_1 region into the surface spin-flop AF_2, phase $[0\rangle$. The first series of spikes, for H between 0.9 and 1.13, is associated with first-order spin-flop transitions, in agreement with Refs. 7,9. For H between 1.13 and 1.32, one observes a second series of transitions associated with the broadening of the discommensuration. Figure 13 shows the susceptibility for the same length of chain ($L=22$) with a smaller anisotropy, $D=0.3$. The spikes are smaller than in Fig. 12 due to a decrease in anisotropy, and some of the surface spin-flop peaks have disappeared, which is what one would expect in view of the critical points along the $[2n\rangle$:$[2n+2\rangle$ phase boundaries noted in Sec. III.

A recent study by Papanicolaou[8] of the dynamics of a model similar to Eq. (1), but with three-dimensional (classical) spins, shows evidence for metastability and hysteresis as the magnetic field H is varied, as one would expect for a first-order SSF transition. Additional hysteresis is seen as the field is increased beyond the SSF transition, consistent with additional first-order transitions of the sort discussed above. Small differences in detail between these results and ours can probably be explained in terms of hysteresis effects, or possibly as due to the fact that the models are not identical. A numerical study of Eq. (1) by Trallori,[9] using an area-preserving map, is also in very good agreement with all of our results, except that certain transitions which we would expect to be first order as the discommensuration moves to the center of the chain and broadens are found to be continuous when D is very small. But this difference is probably not important, since the discontinuities will in any case be very small when D is small, and could be absent because L is finite.

V. ANALYTICAL RESULTS

In this last section we give a detailed derivation of the analytical results presented earlier in the paper. As already noted, analytical solutions to the problem of minimizing the energy are, in general, only available when the spins are in Ising position, $\theta=0$ or π. However, when deviations from these values are small, systematic approximations are possible. Throughout this section we shall use θ_i^0 to indicate Ising or ''locked'' spin values, θ_i for the actual canted val-

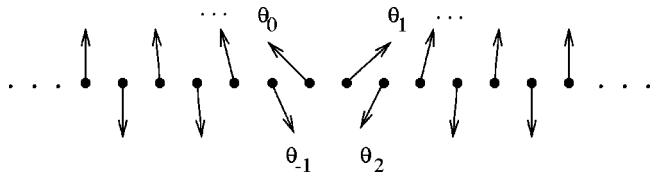

FIG. 14. Schematic representation of the canted discommensuration phase $\langle 2 \rangle$.

ues, and $\tilde{\theta}_i \equiv \theta_i - \theta_i^0$ for the deviations of the latter from the locked values.

To obtain an analytic expression for a second-order boundary separating locked and canted versions of a spin configuration, we start by expanding Eq. (5) to first order in the spin deviations, assuming that they are small,

$$\cos(\theta_i^0 - \theta_{i-1}^0)(\tilde{\theta}_i - \tilde{\theta}_{i-1}) + \cos(\theta_{i+1}^0 - \theta_i^0)(\tilde{\theta}_i - \tilde{\theta}_{i+1}) = [H\cos(\theta_i^0) + D]\tilde{\theta}_i, \tag{14}$$

and then solving these equations self-consistently.

We first apply this strategy to find the boundary separating phases AF′ and $\langle 2 \rangle$, Fig. 2, using the labels for sites in the flopped discommensuration $\langle 2 \rangle$ given in Fig. 14. Equations (14) can be written as recursion relations, in terms of ratios $x_i = \tilde{\theta}_i / \tilde{\theta}_{i-1}$ of successive spin deviations, in the form

$$\begin{gathered} x_{2j}^{-1} + x_{2j+1} = 2 + D + H \text{ for } j \leqslant -1, \\ x_{2j+1}^{-1} + x_{2j+2} = 2 + D - H \text{ for } j \leqslant -1, \\ x_0^{-1} - x_1 = D + H, \\ -x_1^{-1} + x_2 = D + H, \\ x_{2j}^{-1} + x_{2j+1} = 2 + D - H \text{ for } j \geqslant 1, \\ x_{2j+1}^{-1} + x_{2j+2} = 2 + D + H \text{ for } j \geqslant 1, \end{gathered} \tag{15}$$

with a solution

$$\begin{gathered} x_{2j} = s_2 \text{ for } j \geqslant 1, \\ x_{2j+1} = s_1 \text{ for } j \geqslant 1, \\ x_0^{-1} - x_1 = D + H, \\ -x_1^{-1} + x_2 = D + H, \\ x_{2j+2} = s_2^{-1} \text{ for } j \leqslant -1, \\ x_{2j+1} = s_1^{-1} \text{ for } j \leqslant -1, \end{gathered} \tag{16}$$

obtained using techniques of continued fractions. Here s_1 and s_2 are given by

$$\begin{gathered} s_1 = 2[2 + D - H][(2 + D + H)(2 + D - H) + t]^{-1}, \\ s_2 = (1/2)[2 + D + H + t/(2 + D - H)], \\ t := \sqrt{(2 + D + H)^2(2 + D - H)^2 - 4(2 + D + H)(2 + D - H)}. \end{gathered} \tag{17}$$

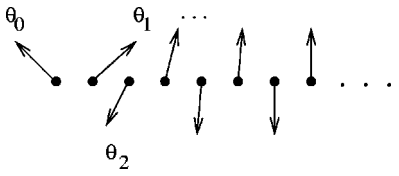

FIG. 15. Schematic representation of the surface phase $[0\rangle$.

The only set of values (H,D) for which Eqs. (16) can be simultaneously satisfied under the constraint that the modulus of s_1 and s_2 cannot exceed 1 (so that the spin deviations decay to zero infinitely far from the discommensuration core) has to satisfy the relation

$$(D + H - 1)^{-1} = 5/3 + D - H, \tag{18}$$

which is the same as Eq. (6). Equation (18) identifies the locus of points where the spin deviations for phase $\langle 2 \rangle$ become vanishingly small, which is the second-order boundary AF′:$\langle 2 \rangle$.

The same method can be used to find the second-order boundary OP between AF_2 and AF_3 in Fig. 6 or 7. In the $[0\rangle$ phase close to the border, with the spins labeled as in Fig. 15, deviations from the corresponding Ising configuration, Eq. (10), will be small, and the solution to Eq. (14) takes the form

$$\begin{gathered} x_{2j} = s_2 \text{ for } j \geqslant 1, \\ x_{2j+1} = s_1 \text{ for } j \geqslant 1, \\ x_1 = 1 - H - D, \\ -x_1^{-1} + s_2 = H + D, \end{gathered} \tag{19}$$

using the same notation introduced previously, with s_1 and s_2 again defined by Eq. (17). These equations yield an additional relation for s_2,

$$s_2 = H + D + [1 - H - D]^{-1}, \tag{20}$$

which can be satisfied together with Eq. (17) only on the locus of points Γ defined by Eq. (12).

A similar analysis assuming small deviations from Ising values for the state $[2\rangle$ shows that the point P on Γ, Fig. 7, occurs at the intersection of the curve

$$1 + D + H = (1 + D - H)^{-1}, \tag{21}$$

with the boundary (18), so that P falls at $H = 4/3$, $D = 2/3$, in good agreement with our numerical results $H = 1.333$, $D = 0.6666$. Likewise, one can show that the other $[2n\rangle$ states for $n > 1$ meet the AF_2 region at P, which is a sort of multicritical point for the surface phase diagram.

A somewhat different approach yields an equation for the boundary between the AF_3 and AF_4 regions, that is, the left edge of the AF_4 region in Figs. 6 and 7. As this corresponds to an accumulation of surface spin-flop states $[2n\rangle$ as $n \to \infty$, the distance from the surface of the chain to the core of the dislocation will become arbitrarily large, so that the spin angles in the discommensuration are essentially independent of distance from the surface,[19,24] as confirmed by our numerical calculations. Hence, by a route analogous to that described in Refs. 19,24, it is possible to evaluate the energy

difference between two neighboring phases, $\Delta E_n = E_{[2n\rangle} - E_{[2n+2\rangle}$, by iterating the equilibrium equations (5) on either side of the discommensuration.

Using the fact that the spin deviations at the surface are becoming vanishingly small, one obtains, to leading order at large n,

$$\Delta E_n \approx \frac{1}{2}(\tilde{\theta}_1 - \tilde{\theta}_0)^2 + \frac{1}{2}(\tilde{\theta}_2 - \tilde{\theta}_1)^2 + \frac{1}{2}D(\tilde{\theta}_1^2 + \tilde{\theta}_0^2) - \frac{1}{2}H(\tilde{\theta}_1^2 - \tilde{\theta}_0^2), \tag{22}$$

where the $\tilde{\theta}_i$'s are the spin deviations of phase $[2n+2\rangle$. The expression for ΔE_n can be simplified by using Eq. (14) to express $\tilde{\theta}_1$ and $\tilde{\theta}_2$ in terms of $\tilde{\theta}_0$, noting that when $i=0$, the term $\cos(\theta_i^0 - \theta_{i-1}^0)(\tilde{\theta}_i - \tilde{\theta}_{i-1})$ must be omitted from Eq. (14), because $i=0$ represents the left edge of the finite chain, Eq. (7). Substituting

$$\tilde{\theta}_1 \approx (1+D+H)\tilde{\theta}_0,$$

$$\tilde{\theta}_2 \approx [2+D-H-(1+D+H)^{-1}]\tilde{\theta}_1, \tag{23}$$

into Eq. (22) gives

$$\Delta E_n = \frac{1}{2}W\tilde{\theta}_0^2 + \mathcal{O}(\tilde{\theta}_0^3),$$

$$W := 2D + 7D^2 + 5D^3 + D^4 + (2D + D^2)H - (1 + 5D + 2D^2)H^2 - H^3 + H^4. \tag{24}$$

Note that this expression holds for all values of D as long as $\tilde{\theta}_0$ is small, that is, the discommensuration is very far from the surface. But this means that an accumulation of states $[2n\rangle$ as n tends to infinity must lie on a locus where W in Eq. (24) vanishes, because in region AF_3 the discommensuration is attracted by the surface $(W>0)$, while it is repelled in $AF_4 (W<0)$. The relevant root of this equation takes the simple form

$$D = \sqrt{1+H^2} - 1, \tag{25}$$

in agreement with Ref. 6, and with our numerical calculations.

VI. CONCLUSIONS

Our work shows that the structure of surface spin-flop (SSF) states and their relationship to the behavior of finite systems is significantly more complex than anticipated in previous work. In particular, the genuine SSF phase for a semi-infinite system, which we identify with region AF_3 in our surface phase diagram, Figs. 6 and 7, has previously been confused with what we call the ''discommensuration'' phase, region AF_4, in which the B-type surface has, strictly speaking, completely disappeared through a restructuring in which a discommensuration has moved infinitely far away from the surface into the bulk. The fact that both the SSF and the discommensuration phase occur at a magnetic field H significantly below that required to produce a bulk spin-flop transition, together with the extremely small interval of H over which the SSF phase is stable when the anisotropy D is small, are no doubt the reasons the two have not been distinguished in previous studies. Nonetheless, they are quite different phenomena, and distinguishing them is essential for a proper understanding of phase transitions associated with surfaces, both in semi-infinite and finite systems.

Our results for the discommensuration and surface phase diagrams lead to very definite and detailed predictions, discussed in Sec. IV, for the complicated sequence of phase transitions occurring in a system with an even number of layers (spins) as H increases at fixed D. They are in good agreement with various numerical studies, including our own, if allowance is made for the uncertainties inherent in numerical work of this sort, and this gives us additional confidence in the validity of our analysis. To the extent that this model antiferromagnet correctly describes Fe/Cr superlattices, we can also claim to have achieved a basic understanding of the processes giving rise to the phase transitions observed experimentally in the latter.

That does not, of course, mean that our model is adequate for understanding SSF phases and other surface phase transitions in more traditional antiferromagnets, such as MnF_2. However, as noted in Sec. I, minimizing the energy of a one-dimensional model is the analog of minimizing the free energy of a three-dimensional layered system, whenever each layer can be described, using mean-field theory or in a purely phenomenological way, by means of a total magnetization serving as a sort of order parameter. To be sure, the parameters which enter the Hamiltonian for the one-dimensional chain may not be those appropriate for three-dimensional system. But one can still expect qualitative similarities in the phase diagrams, even if certain quantitative aspects are different.

In that connection, it is appropriate to ask whether certain features of the discommensuration and surface phase diagrams of the one-dimensional model depend in a sensitive way upon the particular form of the Hamiltonian (1). For example, it contains no spin coupling beyond nearest neighbors, whereas it would be physically more realistic to assume, at the very least, some sort of exchange coupling of further neighbors, decreasing rapidly with distance. Would introducing such interactions lead to significant changes in the phase diagram? Could they, for example, make the SSF phase disappear entirely at low values of the anisotropy?

This is one of many questions which cannot be answered definitively in advance of appropriate calculations. It is worth pointing out that our physical picture of the SSF phase as due to a discommensuration finding its minimum energy at a finite distance from the surface does not seem to depend on the absence of further-neighbor exchange (or possibly other types of) interaction, so we can well imagine that the phenomenon persists with a more realistic Hamiltonian. Nonetheless, this is one respect in which our work remains incomplete. While our numerical results, especially the apparent existence of a nonzero limit for θ_0 as D goes to zero, Fig. 9, support our description in terms of a discommensuration, an appropriate analytic calculation in the limit of small D, of the sort which might (among other things) give the value of this limiting angle, has not been carried out. Such a study would probably provide insight into whether weak further-neighbor interactions simply change the quan-

titative values of various parameters, or lead to a qualitatively different result, such as the absence of the AF_3 region when D is sufficiently small.

It seems unlikely that weak further-neighbor interactions would remove the first-order transitions between the surface phases $[2n\rangle$ and $[2n+2\rangle$, or change the fact that these transitions terminate in critical points as D decreases. On the other hand, such a modification of the Hamiltonian would surely remove the degeneracy of the surface states in the AF_2 region of Figs. 6 and 7. Thus, one would not be surprised to find significant modifications in the phase diagram near the multicritical point P. Indeed, P which might well disappear, to be replaced by some other, more complicated, structure allowing the different $[2n\rangle$ phases to disappear as H increases. Also, sufficiently strong further-neighbor interactions of the proper kind might result in the infinite-chain discommensurations undergoing their broadening transitions at significantly smaller values of the magnetic field H. This could lead to a complicated surface phase diagram in which the minimum energy discommensurations broaden while they are still a finite distance from the surface. How this might effect the $[2n\rangle$ to $[2n+2\rangle$ transitions and their critical points is hard to guess in advance of actually doing a calculation.

Hence, there is much which remains to be understood about surface spin-flop transitions in antiferromagnets. Nonetheless, we believe that the calculations, numerical and analytical, presented in this paper have served to sort out some important physical effects, and in this sense our results provide a solid foundation for future work.

[1] L. Néel, Ann. Phys. (Paris) **5**, 232 (1936).
[2] D. L. Mills, Phys. Rev. Lett. **20**, 18 (1968).
[3] F. Keffer and H. Chow, Phys. Rev. Lett. **31**, 1061 (1973).
[4] R. W. Wang, D. L. Mills, E. E. Fullerton, J. E. Mattson, and S. D. Bader, Phys. Rev. Lett. **72**, 920 (1994).
[5] R. W. Wang and D. L. Mills, Phys. Rev. B **50**, 3931 (1994).
[6] L. Trallori, P. Politi, A. Rettori, M. G. Pini, and J. Villain, Phys. Rev. Lett. **72**, 1925 (1994).
[7] L. Trallori, P. Politi, A. Rettori, M. G. Pini, and J. Villain, J. Phys. C **7**, L451 (1995).
[8] N. Papanicolaou, J. Phys.: Condens. Matter **10**, L131 (1998).
[9] L. Trallori, Phys. Rev. B **57**, 5923 (1998).
[10] C. Micheletti, R. B. Griffiths, and J. M. Yeomans, J. Phys. A **30**, L233 (1997).
[11] F. B. Anderson and H. B. Callen, Phys. Rev. A **136**, 1068 (1964).
[12] S. Aubry, in *Solitons and Condensed Matter Physics*, edited by A. R. Bishop and T. Schneider (Springer-Verlag, Berlin, 1981).
[13] S. Aubry, J. Phys. (Paris) (Paris) **44**, 147 (1983).
[14] S. Aubry, Physica D **7**, 240 (1983).
[15] R. B. Griffiths, in *Fundamental Problems in Statistical Mechanics VII*, edited by H. van Beijeren (Elsevier, Amsterdam, 1990).
[16] L. H. Tang and R. B. Griffiths, J. Stat. Phys. **53**, 853 (1988).
[17] W. Chou and R. B. Griffiths, Phys. Rev. B **34**, 6219 (1986).
[18] K. Hood, J. Comput. Phys. **89**, 187 (1990).
[19] C. Micheletti and J. M. Yeomans, Europhys. Lett. **28**, 465 (1994).
[20] A.B. Harris, C. Micheletti, and J. M. Yeomans, Phys. Rev. Lett. **74**, 3045 (1995).
[21] A.B. Harris, C. Micheletti, and J. M. Yeomans, Phys. Rev. B **52**, 6684 (1995).
[22] N. Papanicolaou, Phys. Rev. B **51**, 15 062 (1995).
[23] L. M. Floria and R. B. Griffiths, Numer. Math. **55**, 565 (1989).
[24] F. Seno and J. M. Yeomans, Phys. Rev. B **50**, 10 385 (1994).